BIOCHEMISTRY
including biophysical chemistry & molecular biology

Article

pubs.acs.org/biochemistry

The Novel Heparin-Binding Motif in Decorin-Binding Protein A from Strain B31 of *Borrelia burgdorferi* Explains the Higher Binding Affinity

Ashli Morgan and Xu Wang*

Department of Chemistry & Biochemistry, Arizona State University, Tempe, Arizona 85287, United States

Supporting Information

ABSTRACT: Decorin-binding protein A (DBPA), a glycosaminoglycan (GAG)-binding lipoprotein found in *Borrelia burgdorferi*, is crucial to the transmission of Lyme disease in its earliest stages. Because of its role in the initial transmission of the disease, DBPA is an ideal target for vaccine development. DBPA sequences from different strains also contain considerable heterogeneity, leading to differing affinities for GAGs and proteoglycans among different DBPA sequences. Through biophysical and structural analysis of DBPA from strain B31, we have discovered a novel and important GAG-binding epitope in B31 DBPA. Removal of the epitope greatly attenuated its affinity for DBPA and may explain the differential GAG affinities seen in DBPAs from other strains of *B. burgdorferi*. Paramagnetic perturbation of the protein with TEMPO-labeled heparin fragments showed bound GAGs are located close to the linker region containing the BXBB motif that plays a significant role in determining the specific affinity and orientation of binding of GAG to DBPA. Thermodynamic contributions of the new motif to GAG binding were also characterized by both nuclear magnetic resonance and isothermal titration calorimetry and compared with those of other DBPA residues previously known to be involved in GAG interactions. These analyses showed the motif is as important as other known binding epitopes. The discovery of the motif offers a possible structural explanation for the previously observed differences in GAG affinities of DBPA variants from different *Borrelia* strains and improves our understanding of DBPA−GAG interactions.

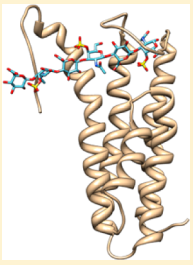

Pathogens often employ surface polysaccharides on host cells as receptors for their initial contacts. Many of them prefer the sulfated polysaccharide glycosaminoglycan (GAG) as their target. So far, GAGs have been shown to be the target of a number of microbes and viruses, including *Mycobacterium tuberculosis*, *Streptococcus agalactiae*, *Plasmodium falciparum*, and herpes simplex virus. These pathogens interact with GAGs through GAG-binding surface proteins, and disruption of these interactions often has an adverse effect on the dissemination of the pathogens and constitutes a new path for the therapeutic treatment of infectious diseases. Among the microbes known to bind GAGs is the bacterium *Borrelia burgdorferi*, the causative agent of Lyme disease. Lyme disease is a common vector-borne illness that can result in symptoms ranging from minor skin rashes to more serious joint, heart, and neural diseases if the disease is not treated. Ticks infected with *B. burgdorferi* transmit the bacterium into the host through bites, and the bacterium colonizes the extracellular matrix.[1] *Borrelia* has been shown to have strong interactions with the matrix, which allows it to move from the vascular system into the surrounding tissues. The spread of the bacterium outside of the vascular system is often a requirement for the advanced stages of the disease and is not easily treated with antibiotics.[1−3] Despite the prevalence of Lyme disease, vaccination against this disease has proven to be difficult because of the genetic variability among the many strains of *Borrelia*.[1,4] A potential therapeutic target is decorin-binding protein (DBP). DBP is a surface lipoprotein that is solely expressed during the human infection stage. DBPs were first identified to adhere primarily to decorin, a small proteoglycan found aligned with collagen in connective tissues, but were later shown to have affinity for proteoglycans containing other types of GAG chains.[5−8] The importance of the DBP−decorin interaction was demonstrated in studies that showed the absence of either decorin or DBPs decreases the effectiveness of the infection process, especially during its early stages.[9−11] Two isoforms of DBP exist in *Borrelia*, commonly termed DBPA and DBPB. While both variants are important for infection, DBPA contains greater sequence heterogeneity than DBPB, which makes it a more challenging therapeutic target.[10−13]

Both *in vivo* and *in vitro* studies have conclusively shown that the GAG segment of decorin is the most biologically relevant binding site for DBPs.[5,14,15] DBPA, in particular, is known to have affinity for a variety of GAGs. In fact, *in vitro* studies have revealed that DBPA binds heparin with greater affinity than other GAGs such as dermatan sulfate (DS) or chondroitin sulfate (CS).[7,14−18] However, DBPA's binding affinity for GAGs seems to differ wildly among different *Borrelia* strains. The most in-depth study of the correlation between DBPA sequence variation and its activity was conducted by Benoit et al.[16] They looked at the GAG affinity of strains B31, 297, N40, and B356 of *B. burgdorferi* and strain PBr of *Borrelia garinii* and strain VS461 of *Borrelia afzelii*. It was evident from the binding assays that DBPA from PBr possessed the highest binding affinity for GAGs. This is not surprising because this strain's DBPA contains the largest number of basic amino acids as well as the highest ratio of basic amino acids to acidic amino acids

Received: June 2, 2013
Revised: October 22, 2013
Published: October 22, 2013

   dx.doi.org/10.1021/bi401376u | *Biochemistry* 2013, 52, 8237−8245

among all strains investigated in the report. However, despite the high degree of sequence homology among the four *B. burgdorferi* strains, B31 and 297 versions of DBPAs possessed a much higher affinity for GAGs than N40 and B356.[16] Because of DBPA's role as an extracellular matrix (ECM) adhesin, its GAG binding affinity may be a crucial determinant in *Borrelia* infectivity, making understanding the molecular mechanism underlying its interactions with GAGs a priority. Furthermore, the void in our knowledge of GAG−protein interactions in general means DBPA's sequence-dependent GAG affinity is an excellent opportunity to investigate principles governing GAG−protein interactions. However, there is yet no molecular explanation for the large deviations observed in GAG binding affinities of DBPAs from four different strains of *B. burgdorferi*.

Attempts to identify GAG-binding epitopes of DBPA started soon after the protein's discovery. Using sequence alignment and a peptide screening approach, Hook and co-workers first identified residues K82, K163, and K170 as being critical to the decorin binding ability of DBPA.[19] More recently, Benoit et al. serendipitously discovered that the absence of the C-terminus of DBPA from strain VS461 (last 11−13 residues of DBPA) abrogated the protein's ability to bind GAGs.[16] Unfortunately, because these motifs are shared among most strains of *B. burgdorferi*, they do not reveal the structural rationale behind differing GAG affinities between strains B31 and N40. However, the recently determined structure of B31 DBPA does give one clue about the reason behind B31's enhanced GAG affinity: according to the structure, the proposed GAG-binding epitope on B31 is a basic pocket consisting of helices and two dynamic segments of DBPA. Previously identified GAG-binding motifs are all found in the pocket (Figure 1).[17] Most intriguingly, one of the flexible segments, a linker between helices 1 and 2 covering the pocket (residues 58−72), contains a BXBB motif (B represents a basic amino acid) not seen in many versions of DBPA, including those from strains N40 and B356.

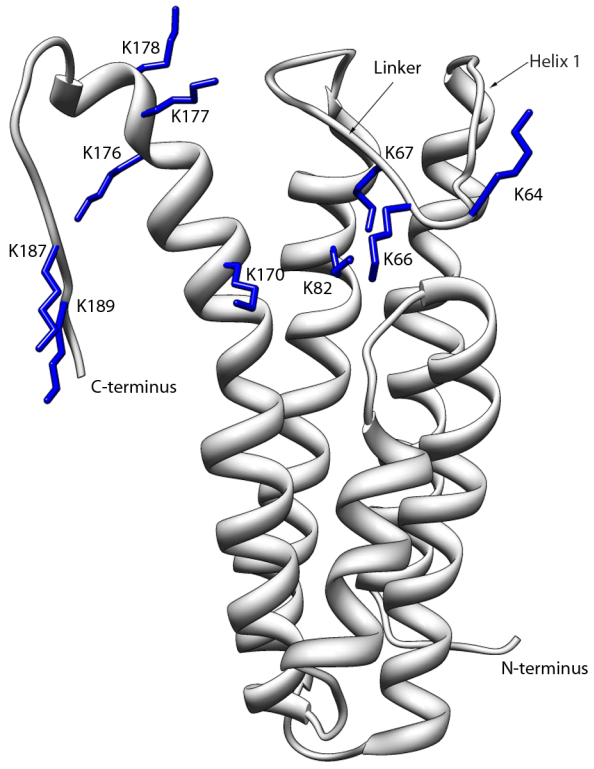

Figure 1. Ribbon depiction of wild-type B31 DBPA with the side chains of the mutated lysine residues colored blue.

Guided by the structure for B31, we are now able to propose a hypothesis explaining the differences in GAG affinities of DBPAs from strains B31 and N40. In particular, we believe the linker BXBB motif may be significantly important in promoting DBPA−GAG interactions. In this work, we report the biophysical and structural characterization of the interactions between size-defined GAG fragments and known GAG-binding motifs on B31 DBPA. Our choice of GAG ligands is size-defined low-molecular weight heparin. This decision is prompted by the fact that DBPA has a very low affinity for low-molecular weight DS *in vitro*, which made accurate characterizations of DBPA's GAG affinity impractical.[20] Heparan sulfates, a form of heparin that resides on the epithelial cell surface, are known to act as receptors for *B. burgdorferi*,[7] and given the promiscuity of most GAG-binding proteins, epitopes identified with heparin should be applicable to the binding of other types of GAGs. Through the use of fluorescence-assisted gel mobility shift assays (GMSAs), we showed the BXBB cluster in the linker is vital to the GAG affinity of B31 DBPA, such that B31 DBPA's affinity for both low-molecular weight heparin and DS decreases significantly in its absence. The free energy contribution of each motif to GAG binding was also quantitatively characterized using nuclear magnetic resonance (NMR) and isothermal titration calorimetry (ITC), and the result correlated well with those observed in gel mobility shift assays. In particular, the linker BXBB motif and the three lysine residues on the helices contributed most to the free energy of binding, and the C-terminal residues contributed much less. ITC results also revealed that the interaction is driven almost entirely by favorable enthalpic changes. The direct interaction of the linker residues with GAGs was confirmed through a NMR paramagnetic relaxation enhancement (PRE) study using a novel TEMPO-tagged paramagnetic heparin ligand. The results unambiguously proved that the linker bound not only heparin but also the heparin fragment oriented specifically with the reducing end of the fragment close to the linker. Using observations in this study, a rationale for the higher GAG affinity seen in B31 DBPA can now be offered along with a structural model for the interactions between GAG fragments and B31.

EXPERIMENTAL PROCEDURES

Expression and Purification of B31 Variants. The open reading frame for the wild-type (WT) mature B31 DBPA (residues 24−191) was synthesized by Genscript Inc. (Piscataway, NJ) and cloned into the pHUE vector that incorporates His-tagged ubiquitin at the N-terminus of B31 to give a fusion protein.[21] Mutagenic primers were designed for four B31 mutants: ^{64}KDKK^{67} to ^{64}SDSS^{67}, ^{176}KKK^{178} to ^{176}SSS^{178}, ^{187}KCK^{189} to ^{187}SCS^{189}, and K82,170S. The forward primers for the mutants were as follows: ^{64}SDSS^{67}, 5′-GCGGTTAACTTCGATGCCTTCAGCGATAGCAGCACCGGCAGTGGTGTGAGCGAAAATCCG-3′; ^{176}SSS^{178}, 5′-CAAAAACTACTGCACGCTGAGCAGCAGCGAAAATAGCACCTTC-3′; ^{187}SCS^{189}, 5′-GCACCTTCACGGATGAAAGCTGTAGCAACAATTGAAAGCTTAG-3′; K82S, 5′-CCGTTTATCCTGGAAGCCAGCGTGCGTGCAACCACG-3′; K170S, 5′-CTGCAGCGCGTGCATACCAGCAACTACTGCACGCTG-3′. Mutagenesis was conducted with the Agilent Quickchange site-

directed mutagenesis kit by following the manufacturer's instructions, and the incorporation of the mutations was confirmed though sequencing.

To express the protein, the plasmid was transformed into *Escherichia coli* BL21(DE3) and the bacteria were grown at 37 °C in M9 medium to an OD_{600} of 0.5. The M9 medium was supplemented with $^{15}NH_4Cl$ and/or [^{13}C]glucose depending on the desired isotopic labeling scheme. The bacteria were induced with 0.5 mM IPTG and incubated overnight at 30 °C. The cells were harvested via centrifugation, and the resuspended cell pellet was incubated with 1 mg/mL lysozyme and then sonicated to lyse the cells. The fusion protein in the supernatant was obtained via Ni affinity chromatography using a 1 mL HisTrap column (GE Life Sciences). The fusion protein was eluted off the column using an imidazole gradient from 35 to 500 mM at a flow rate of 1 mL/min. The fusion protein was exchanged into 25 mM Tris (pH 8.0) and 100 mM NaCl and digested with USP2 and 1 mM DTT overnight at room temperature.[21] The cleaved DBPA was purified using a 1 mL HisTrap column. The cleaved DBPA was found in the flow-through, which was collected and concentrated. Figure 1 of the Supporting Information shows the SDS–PAGE analysis of the sample during each stage of purification.

Production of Heparin and TEMPO-Labeled Heparin Fragments. Heparin and DS purchased from Sigma-Aldrich were first dialyzed and lyophilized to remove excess salt. Porcine mucosa heparin was digested with 0.5 IU of heparinase I (IBEX Inc.), and DS was digested with Chondroitinase ABC (Sigma-Aldrich) until the depolymerization was 30% complete to give short fragments.[22] The fragments were separated using a 2.5 cm × 175 cm size exclusion chromatography column (Bio-Rad Biogel P10) with a flow rate of 0.2 mL/min. The fractions containing the same size were pooled, desalted, and lyophilized. No further steps were taken to separate fragments bearing different sulfation patterns. Disaccharide analysis of the fragments used showed that heparin fragments contained ~45% disulfated disacharrides and ~40% trisulfated disaccharides and DS contained mostly monosulfated disaccharides. For the PRE study, the reducing end of heparin hexasaccharide (dp6) fragments was modified using a nitroxide radical, 4-amino-TEMPO, through reductive amination (Figure 2 of the Supporting Information). Specifically, 300 μM TEMPO was incubated with 1 mg of the heparin fragment and 25 mM $NaCNBH_3$ at 65 °C in water for 3 days. The mixture was then desalted, and GAG fragments were isolated using SAX–HPLC.

Gel Mobility Shift Assays for WT B31 and B31 Mutants. Heparin decasaccharides (dp10), heparin hexasaccharides (dp6), and DS hexasaccharides were fluorescently labeled with 0.1 M 2-aminoacridone (2-AMAC).[23] Briefly, 5 μL of 20 mg/mL GAG fragment was mixed with 40 μL of 0.1 M 2-AMAC that had been dissolved in 85% Me_2SO and 15% glacial acetic acid. This mixture was incubated at room temperature for 15 min before 40 μL of 1.0 M $NaCNBH_3$ (in deionized water) was added. The fragments were incubated at 37 °C overnight and then precipitated by adding 9 volumes of ethanol and incubating the mixture at −20 °C for 15 min. After centrifugation, the pellet was washed with an additional 9 volumes of ethanol, and the resulting pellet was resuspended in 50 mM sodium phosphate (pH 6.5) and 150 mM NaCl. To perform the gel mobility shift assays, 1 μg of the fluorescently labeled heparin fragment was mixed with 0.5, 1, or 2 molar equiv of WT B31 or B31 mutants in 50 mM sodium phosphate (pH 6.5) and 150 mM NaCl buffer. For the DS dp6 GMSA, the fluorescently labeled fragments were mixed with the protein at a DS:protein ratio of 3, and in 50 mM acetate (pH 5) and 150 mM NaCl buffer. The control is the same mixture but with an equal volume of the same buffer without the protein. The reaction mixtures were incubated at room temperature for 30 min and were run at 120 V for 15–25 min in a 1% agarose gel immersed in the same buffer as the buffer used for incubation. A UV panel was used to visualize the shifts.[24]

Titrations of WT and Mutant B31 Using Heparin dp6. K_D values of the interaction between heparin dp6 and B31 were estimated using NMR-monitored titration. Specifically, 2.10 mM heparin dp6 was added to 400 μL of 150 μM DBPA in 300 μM aliquots. This was done for B31 WT, B31 ^{64}SDSS^{67}, B31 ^{187}SCS^{189}, and B31 K82,170S. For B31 ^{176}SSS^{178}, 3.60 mM heparin dp6 was added to 150 μM DBPA in 600 μM aliquots. The pH of all the protein samples was lowered from 6.5 to 5.0. A ^{1}H–^{15}N HSQC spectrum was collected at each titration point. The chemical shift changes in the ^{1}H and ^{15}N dimensions were normalized into one chemical shift value.[25] The normalized chemical shift was calculated using the equation $\delta_H = [\Delta\delta_H^2 + (1.7\Delta\delta_N)^2]^{1/2}$, where δ_H and δ_N represent the chemical shifts for ^{1}H and ^{15}N, respectively. The K_D of binding was extracted using the fitting feature in xcrvfit (http://www.bionmr.ualberta.ca/bds/software/xcrvfit/) to plot the normalized chemical shift against the ligand:protein ratio. Data for the titrations were collected on Bruker Ultra-Shield 600 and 850 MHz spectrometers.

Isothermal Titration Calorimetry of DBPA–Heparin Interactions. ITC of DBPA and DBPA with heparin dp6 was performed on a Microcal ITC-200 calorimeter. Samples consisting of 300 μL of 200 μM DBPA were titrated with aliquots of a 10 mM heparin dp6 stock solution at 25 °C. Buffer containing no protein was used as a reference. Each titration was repeated three times, and average values of the dissociation constant and enthalpy change (ΔH) are reported.

Acquisition and Analysis of Backbone Dynamics Data. All NMR samples consisted of 400 μL of 150–200 μM ^{15}N-labeled B31 WT DBPA in 50 mM NaH_2PO_4 (pH 6.5) and 150 mM NaCl buffer. NMR data for relaxation spectra were collected on Bruker Ultra-Shield 600 and Varian Inova 800 MHz spectrometers. Paramagnetic relaxation enhancement (PRE) from TEMPO-labeled heparin fragments was quantified by measuring ^{1}H T_2 values of the backbone amide protons according to the method of Iwahara et al.[26] before and after the radical on the heparin fragment was reduced with ascorbic acid. Relaxation delays of 1, 4.5, 8, 11.5, 15, and 18.5 ms were used. The difference in the ^{1}H T_2 before and after reduction of the radical is the relaxation contribution from the TEMPO radical. T_1, T_2, and steady state heteronuclear nuclear Overhauser effect (NOE) experiments were conducted for WT B31 in the presence and absence of 24 molar equiv of heparin dp6. The relaxation delays for the T_1 experiments were 0.1, 0.3, 0.5, 0.7, 0.9, and 1.3 s. The relaxation delays for the T_2 experiments were 10, 30, 50, and 70 ms. Steady state heteronuclear NOEs were derived from peak intensity ratios of spectra collected with and without proton saturation for 3 s. The data were processed with NMRPipe[27] and analyzed using NMRView.[28] The order parameter S^2 was extracted using the model-free approach with relax, model-free software.[29] The protein is assumed to undergo isotropic global rotational diffusion, and its global rotational correlation time, τ_m, was estimated as the average rotational correlation times of all residues in the structured region. The residue-specific correlation times were calculated according to

eq 9 of Kay et al.,[30] taking into consideration only contributions from $J(0)$ and $J(\omega_N)$. In particular, the equation $\tau_c = 1/(4\pi\nu_N) \times [6(T_1/T_2) - 7]$ was used, where ν_N is the resonance frequency of ^{15}N in hertz. DBPA's internal motions were characterized through the fitting of parameters S^2 (magnitude of internal motion), τ_e (internal motion correlation time), and R_{ex} (contribution of conformational exchange to transverse relaxation) for each backbone amide nitrogen atom.

RESULTS

Interaction of B31 Mutants with GAGs. To assess the importance of known B31 DBPA GAG-binding motifs to GAG interactions, we created four B31 mutants each lacking a basic amino acid cluster from one of the proposed GAG-binding motifs. The linker mutant ^{64}SDSS^{67} contains the mutations of residues ^{64}KDKK^{67} in the linker to ^{64}SDSS^{67}. The ^{176}SSS^{178} mutant contains the mutations of C-terminal residues ^{176}KKK^{178} to ^{176}SSS^{178}. Similarly, the ^{187}SCS^{189} mutant contains the mutations of C-terminal residues ^{187}KCK^{189} to ^{187}SCS^{189}. Finally, the K82,170S mutant contains the mutations of two helical residues first identified as being part of the GAG-binding epitope.[19,31] Because native polymers of GAGs induce only signal disappearance when added to samples of DBPA,[20] uniform-sized fragments of GAGs were used to evaluate mutagenesis-related changes in DBPA's GAG affinity. Furthermore, heparin hexasaccharide (dp6) was chosen as the primary ligand. The choice is a consequence of DBPA's relatively strong affinity for heparin. Similarly sized fragments of both DS and CS, the GAG types found on decorin, do not interact strongly with DBPA even under the most optimized conditions.[14,16,20]

A qualitative characterization of B31–heparin interactions was first conducted with a gel mobility shift assay and fluorescently labeled heparin dp10 fragments.[24] The gel mobility shift assay is based on the principle that the migration of the heparin fragments is greatly impeded when proteins are bound. The effect is a combination of an increase in the apparent size of the complex and a reduction in the net charge of the complex. Using such an assay, we measured the GAG affinity of wild-type B31 as well as the linker mutant ^{64}SDSS^{67}, C-terminal mutants ^{176}SSS^{178} and ^{187}SCS^{189}, and helical mutant K82,170S. The results are shown in Figure 2. The assay clearly demonstrated that WT B31 is capable of inducing shifts in a significant proportion of the heparin fragments. However, the four B31 mutants did not have a similarly strong effect on heparin fragment migration (Figure 2). ^{64}SDSS^{67} and K82,170S mutants showed no shift of the heparin fragment, while ^{176}SSS^{178} and ^{187}SCS^{189} induced minor shifts of the heparin fragment. These observations support the previous studies indicating the importance of lysine residues in binding GAGs. However, the linker BXBB motif and the helical lysine residues contribute more to DBPA B31's GAG affinity than the C-terminal basic clusters. Differences in GAG affinity also exist among the C-terminal clusters. Specifically, the ^{176}SSS^{178} mutant has a larger effect on binding than the ^{187}SCS^{189} mutant. Similar trends were seen with heparin dp6 (Figure 3 of the Supporting Information), although its interactions with the C-terminal mutants of ^{176}SSS^{178} and ^{187}SCS^{189} are not readily visualized as in heparin dp10, indicating the binding affinity of DBPA for heparin dp6 may be weaker. The same assay was also conducted with DS dp6 (Figure 4 of the Supporting Information). However, its weak affinity for DBPA

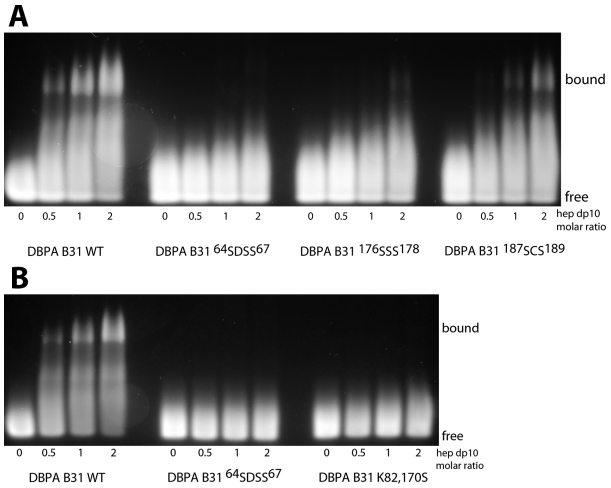

Figure 2. Gel mobility shift assay of heparin dp10 in the presence of increasing concentrations of (A) WT B31, ^{64}SDSS^{67}, ^{176}SSS^{178}, and ^{187}SCS^{189} and (B) WT B31, ^{64}SDSS^{67}, and K82,170S.

demanded the use of conditions more conducive to protein–GAG interactions. In particular, the assay was conducted at pH 5 and at a GAG:protein ratio of 3. Under these conditions, some DS binding can be seen for the wild type and the ^{187}SCS^{189} mutant. However, the other three mutants showed no sign of binding DS dp6. This is consistent with what has been observed with heparin fragments, indicating DBPA's interactions with DS and heparin are governed by similar factors.

Thermodynamic Contributions of the GAG-Binding Motifs. Titrations were conducted with heparin dp6 on the WT and mutant forms of B31 to quantitatively measure the thermodynamic contribution of each motif to GAG binding. Because GAG–protein interactions are highly dependent on the size of the GAG polymer, B31 DBPA's affinity for heparin dp6 is weak at physiological pH ($K_D \sim 4$ mM). Such weak affinity made detections of affinity changes difficult. As a result, the titrations were repeated at pH 5.0, a pH that produced more favorable electrostatic surface potentials for binding, thus increasing the affinity of DBPA for heparin. Furthermore, the pH change did not change the pattern of peaks or the peak migration direction significantly, indicating DBPA–heparin interactions were not greatly perturbed. With the lower pH, binding of heparin dp6 to WT B31 went from a K_D of 4 mM to a K_D of 0.5 mM (Figure 3). The shifts of two C-terminal residues (E186 and N191) showing the largest migration distances were used to determine the K_D of the interaction for each DBPA variant. The only exception was mutant K82,170S, for which A54 was used in place of E186 because of the poor signal:noise ratio of the E186 peak. Table 1 lists the K_D values derived from N191 and E186 for each B31 variant. It is noteworthy that K_D values obtained using E186 chemical shift migrations are consistently lower than those from N191. This most likely reflects the flexibility of the C-terminus as a binding site and the fact that acidic amino acids are more likely to repel the negatively charged GAG ligands, thus providing a higher K_D. However, these E186-derived K_D values reflect the same trend of decreasing affinities among the mutants examined that those of N191 do. Compared to the binding K_D of 0.5 mM for the wild type, the linker mutant ^{64}SDSS^{67} exhibited a much higher K_D. An accurate value of the K_D for the ^{64}SDSS^{67} mutant could not be obtained under the current experimental conditions but is estimated to be >20 mM. The K_D values

dx.doi.org/10.1021/bi401376u | Biochemistry 2013, 52, 8237–8245

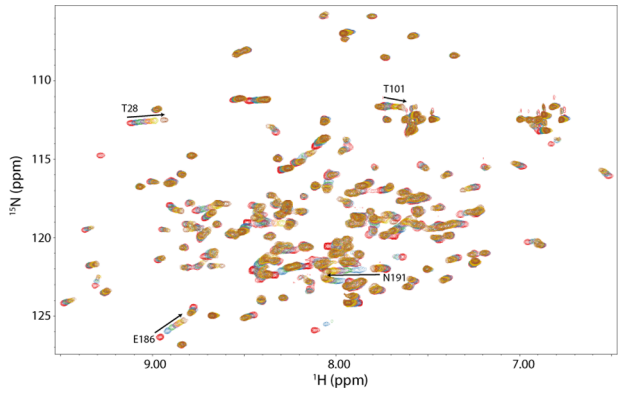

Figure 3. ^{1}H—^{15}N HSQC overlays of WT B31 DBPA in the presence of increasing concentrations of heparin dp6. Signals experiencing a large migration (E186 and N191) are indicated with the residue number and direction of migration. The red contour represents the initial HSQC spectrum of DBPA in the absence of heparin dp6. Each subsequently colored contour represents the HSQC spectrum of DBPA at different concentrations of heparin dp6. The concentrations of heparin dp6 were 0.3, 0.6, 0.9, 1.2, 1.5, and 2.4 mM. The concentration of DPBA was 0.15 mM.

Table 1. K_D Values of DBPA−Heparin dp6 Interaction from Calculation Using Chemical Shift Changes from Residues E186 and N191 of DBPA B31 Variants and from ITC

	K_D (mM)		
	N191	E186	ITC
WT	0.55 ± 0.04	0.76 ± 0.04	0.75 ± 0.03
^{64}SDSS^{67}	>20	>50	∼5.2 ± 0.8
K82,170S	4 ± 1	—	∼11 ± 3
^{176}SSS^{178}	2.5 ± 0.5	3.3 ± 0.7	—
^{187}SCS^{189}	0.85 ± 0.06	2.0 ± 0.3	—

for helical mutant K82,170S and C-terminal mutants ^{176}SSS^{178} and ^{187}SCS^{189} were approximately 4, 2.5, and 0.85 mM, respectively. The binding curves for all samples are included in Figure 5 of the Supporting Information. On the basis of these dissociation constants, the ΔG contributions of the BXBB motif in the linker were calculated to be more than 2.7 kcal/mol while the K82,K170 motif and the C-terminal ^{176}SSS^{178} motif contribute only 1.2 and 1 kcal/mol, respectively. The ^{187}SCS^{189} motif contributes very little thermodynamically to GAG binding. A summary of the results is presented in Table 1.

To confirm the NMR observations and shed further light on the thermodynamic driving force of DBPA−GAG interactions, we also performed ITC analysis of the interactions between heparin dp6 and WT DBPA as well as two weaker binding mutants, ^{64}SDSS^{67} and K82,170S. The ITC results agreed well with the NMR findings. In particular, ITC found the K_D for the complex of WT B31 DBPA with heparin dp6 to be ∼0.8 mM. Estimations from ITC about the K_D of the interactions of heparin dp6 with the ^{64}SDSS^{67} mutant and the K82,170S mutant are less precise because of limitations on the concentrations of both the heparin dp6 stock solution, which produced a high dilution heat at high concentrations, and the mutants, but both titrations showed clear signs of significant increases in their K_D values. The K_D of interactions of heparin dp6 with the ^{64}SDSS^{67} mutant is estimated to be ∼5 mM. The K_D for the K82,170S mutant is estimated to be ∼10 mM (Table 1 and Figure 6 of the Supporting Information). These results agree with the trend obtained using GMSA and NMR. Furthermore, similar to those of other carbohydrate-binding proteins,[32] DBPA's interaction with heparin dp6 is mostly driven by favorable enthalpic changes, which is estimated to be approximately −4.8 kcal/mol. Entropic changes were small but unfavorable, contributing approximately 0.5 kcal/mol to the free energy change. Figure 6 of the Supporting Information shows the ITC titration curve of the WT as well as ^{64}SDSS^{67} and K82,170S mutants with heparin dp6.

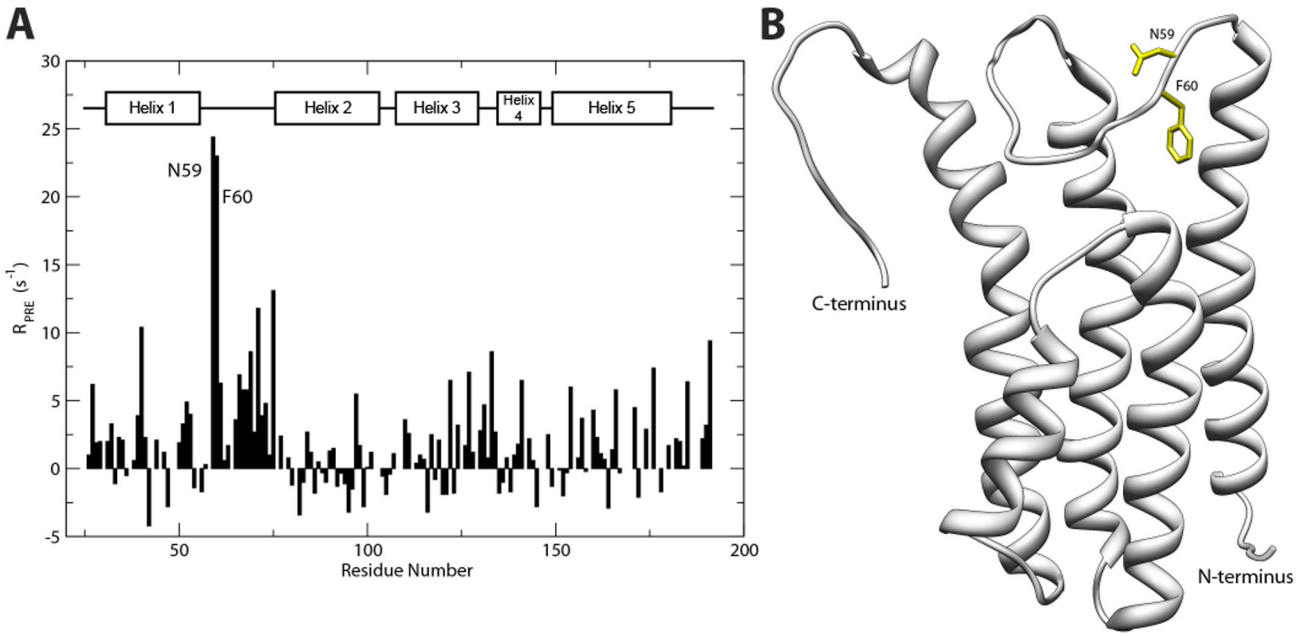

Figure 4. (A) Comparison of the residue-specific PRE effect on the backbone amide proton from TEMPO-labeled heparin dp6 before and after reduction of the TEMPO radical. The comparison indicated that two residues (N59 and F60) experienced a greater PRE effect when probed with the TEMPO radical. (B) Ribbon depiction of WT B31 DBPA with the residues experiencing the greatest PRE effect colored yellow.

dx.doi.org/10.1021/bi401376u | *Biochemistry* 2013, 52, 8237−8245

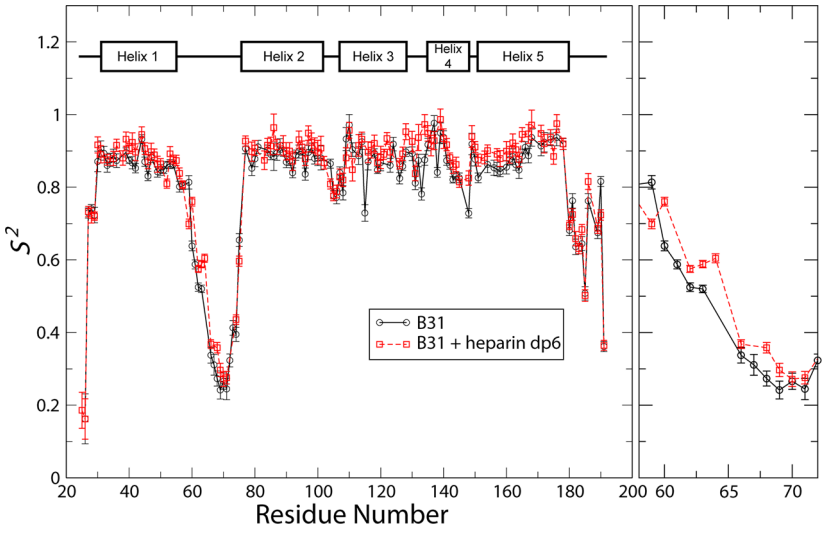

Figure 5. Order parameters of backbone amide nitrogen atoms for WT B31 DBPA in the absence (—) and presence (---) of 24 molar equiv of heparin dp6. Details of order parameter changes for residues in the first half of the flexible linker are shown in the right panel.

Specific DBPA–GAG Interactions Using Paramagnetically Labeled GAG Ligands. In our previous characterization of B31 DBPA structure, indirect indications of the flexible linker's role in contacting GAGs were already evident. In particular, NMR chemical shifts of atoms in linker residues underwent significantly larger changes than residues in other parts of the protein, and amide protons of residues G69, S70, and G71 saw dramatic decreases in solvent exchange rates in the presence of heparin dp6.[20] To obtain direct evidence that the linker is close to the bound GAG, we probed B31 DBPA with a novel paramagnetic heparin dp6 ligand. The paramagnetic functional group used in this study is TEMPO, a stable nitroxide radical that has commonly been used as a structural probe in solution NMR. The paramagnetic effect of TEMPO stems from the unpaired electron that generates an inhomogeneous magnetic field in its vicinity, causing NMR signals of nearby atoms to experience larger longitudinal and transverse relaxation rates, leading to signal broadening. Such an effect is termed paramagnetic relaxation enhancement (PRE). Because PRE is distance-dependent, the residues closest to the radical will experience the greatest increases in relaxation rates, which can be quantitatively measured.[26] TEMPO-tagged glycans have been used previously to probe protein–glycan interactions.[33,34] However, there is no report of location-specific TEMPO labeling of GAG fragments for the purpose of studying protein–GAG interactions. For this study, we constructed a novel TEMPO-labeled heparin dp6 derivative by attaching 4-amino-TEMPO specifically to the reducing end of the heparin dp6 fragment using reductive amination (Figure 2 of the Supporting Information). Although reductive amination has been used to attach fluorescent tags to heparin, this is the first report of stable radical functionalization of heparin using reductive amination. To accurately quantify the size of the PRE on each residue, the amide proton transverse relaxation rates were measured in the presence of 6 molar equiv of TEMPO-labeled heparin dp6 before and after reducing the TEMPO radical with ascorbic acid. The difference in the two relaxation rates is due entirely to the PRE from the nearby radical. This allowed the location of the reducing end of heparin to be accurately determined. Figure 4A shows the residue-specific PRE of each backbone amide proton. The residues that showed the most perturbation after the radical was reduced were N59 and F60, both of which showed a rate decrease of >20 s^{-1}. Figure 7 of the Supporting Information shows the HSQC peaks of the two residues in the presence of the oxidized and reduced radical as well as the normalized intensity decay curve from which the relaxation rates were calculated. These residues are positioned at the N-terminal end of the linker and close to the BXBB motif. Their perturbation indicates the radical was positioned near the BXBB epitope in the linker. Because the radical was specifically attached to the reducing end of the heparin fragment, the PRE data imply that the reducing end of the fragment is present near the BXBB epitope, as well. These data provide direct confirmation that the BXBB motif is part of the GAG-binding site of DBPA. It is also noteworthy that other basic amino acid clusters in the protein showed minimal perturbation by the TEMPO-labeled heparin. However, this may be because these residues interact only with regions of heparin distant from the reducing end. To confirm the PRE effect is not the result of nonspecific TEMPO–DBPA interactions, the protein was also titrated with 4-amino-TEMPO at similar protein:ligand ratios, and no significant changes in the transverse relaxation rates of the protein were observed.

Backbone Dynamics of B31 DBPA. Because both the linker and the C-terminus of DBPA are quite flexible, the possibility of GAG-induced changes in backbone dynamics of the protein exists. To quantify these changes, the popular Model-Free approach was used to estimate the extent of picosecond to nanosecond time scale internal motions in the protein.[35,36] This technique allowed the magnitude of internal motions of the atoms to be represented by the simple order parameter S^2. Furthermore, its value can be estimated using measurable NMR observables such as longitudinal and transverse relaxation rates and steady state heteronuclear NOE.[30] These observables were measured on the backbone amide nitrogen atom using established NMR experiments, and the experimental data were fit using relax[29] to obtain residue-specific order parameters. The fitting assumes the protein undergoes isotropic global rotational motion, which is usually true for well-folded globular proteins. To perform the fitting, the global rotational correlation time (τ_m) of the protein was

dx.doi.org/10.1021/bi401376u | *Biochemistry* 2013, 52, 8237–8245

estimated using transverse and longitudinal relaxation rates of residues located in the structured parts of the protein. In the absence of heparin dp6, τ_m was estimated to be ~12.5 ns. After 24 equiv of heparin dp6 had been added, τ_m increased slightly to 14.2 ns. Figure 5 shows the order parameters of backbone amide nitrogen atoms of WT B31 in the presence and absence of 24 equiv of heparin dp6. An order parameter value of 0 indicates a complete lack of internal order, while a value of 1 indicates the atom is perfectly rigid relative to other atoms and experiences no internal motion. The values of order parameters for the structured parts of the protein are around 0.85 (Figure 5). No large changes in order parameters were observed for the heparin-containing sample. However, some reductions in order parameters were observed for residues in the first half of the linker. In particular, residue F60, which is one of two residues greatly perturbed by the paramagnetic ligand, showed an increase of ~0.15 in its S^2 value after heparin dp6 had been added. These measurements indicate the presence of heparin dp6 did not change the magnitudes of DBPA's fast time scale motions significantly. The lack of large scale changes in protein dynamics is consistent with ITC measurements, which showed entropic contributions to binding are small. To ensure the accuracy of the fitting, contributions to observed relaxation rates from microsecond to millisecond time scale conformational exchange (R_{ex}) were also estimated in the model. However, no significant contributions from motions on these time scales were seen.

DISCUSSION

Since the discovery of DBPA, its role in the development of Lyme disease has been extensively studied.[10−12,37] It has been shown to be important in the establishment of infection in early stages of the process and may act by both anchoring bacteria to the extracellular matrix and modulating the immune system response to the bacterium.[11] One aspect of DBPA's activity that has not been fully explored is the relationship between variations in its sequences and its activity as an adhesin. In particular, a previous study revealed that DBPAs from strains B31 and 297 of *B. burgdorferi* possessed much higher GAG affinities than strains N40 and B356 despite a high level of sequence homology among them.[16] Our results offer a possible explanation for the observations: both B31 and 297 DBPAs contain the BXBB motif in the linker, whereas in N40 and B356, the motif is substituted with the sequence TDSE (Figure 8 of the Supporting Information), making the net charge for the cluster −2 rather than +2. This effectively prevented strong interactions between the linker and GAGs. Besides the changes in the linker, N40 and B356 strains of DBPA are also devoid of residues equivalent to K124 and K128 of B31. However, these residues are not located in the binding pocket and have not been perturbed significantly in either chemical shift mapping or the PRE experiments and, thus, may not play a significant role in GAG binding. The fact that DBPA from strain 297 has a high affinity for GAGs despite not having a residue equivalent to K128 also partially confirms the hypothesis. The differences in GAG binding affinity between B31 and N40 DBPAs cannot be attributed to a lack of basic amino acids in N40 DBPA either: N40 has a number of basic amino acids in its version of DBPA comparable to the number in B31's version (27 basic amino acids in N40 vs 29 in B31) as well as a basic:acidic residue ratio (1.08) similar to that of B31 (1.07). Therefore, the lack of the BXBB motif could be a major factor in N40 DBPA's lower GAG affinity. In fact, this variation in DBPA sequence could be a significant contributing factor to the observed lower binding efficiency to host cells by the N40 strains of *Borrelia*.[38] An analysis of all DBPA sequences from *B. burgdorferi* available in the UniProt database showed that of 20 available sequences, seven possessed the BXBB motif, indicating the GAG-binding enhancing epitope is not exclusive to strains B31 and 297.

In this work, the role played by the BXBB motif in GAG binding has been experimentally verified using paramagnetically tagged GAG ligands. In addition to providing confirmation of interactions between the BXBB motif and GAGs, results from the titration of DBPA by the paramagnetic ligand are surprising in that they show DBPA's interaction with GAGs may be highly orientation-specific. The fact that only residues in the linkers experienced significant PRE indicates the reducing end of the ligand is close to the linker. However, the C-terminus, which is located at the opposite side of the binding pocket, may not be. An alternative explanation is that the affinity of the C-terminus for GAGs is weaker and, therefore, may not be affected by PRE to the same extent as the linker residues when the reducing end is close to it. Consequently, the binding mode with the fragment in the opposite orientation may not be detected by PRE. It is also unclear whether the specificity is a consequence of the opening of the reducing end monosaccharide during reductive amination. The increased flexibility due to the linearization of the sugar may have artificially increased the affinity of the pockets for the reducing end. However, if the observation is not the result of an artifact, it shows DBPA's interactions with GAGs are highly specific and may be the result of close geometric matching between sulfate groups on GAGs and basic amino acids in DBPA.

Characterization of the DBPA's backbone dynamics showed conformational entropy does not appear to be a significant factor in determining the binding affinity. This agrees with the small entropic change measured in ITC. The fact that one of the most flexible segments of the protein also contains a crucial GAG-binding epitope is demonstrative of the dynamic nature of DBPA−GAG interactions and lends a plausible explanation for the weak interaction of DBPA with GAGs. However, despite the millimolar dissociation constants for these interactions, the interaction is by no means irrelevant. The dissociation constants measured in this study pertain to only low-molecular weight heparin fragments. However, it is well-known that the affinity of proteins for GAGs is highly dependent on the size of GAGs. Longer GAG polymers *in vivo* will have a much higher affinity for DBPA than the hexasaccharide used in this study because of the effects of avidity. This does not imply the use of short GAG fragments as the ligand is not relevant. The size of the GAG-binding pocket on DBPA can accommodate only one hexasaccharide at a time; therefore, hexasaccharides are the right size to achieve sufficient affinity without the risk of promoting protein oligomerization. Size-defined GAG fragments also allowed for a more objective evaluation of DBPA's preferences for different GAG types. In fact, such weak interactions are by no means extraordinary in protein−carbohydrate interactions.[39] Specifically, the well-studied interactions between the influenza A viral hemagglutinin monomer and its sialyated *N*-glycan receptor possess dissociation constants in the millimolar range,[40] as does the interaction between high-mannose *N*-glycan and the immune receptor DC-SIGN.[41] These weak interactions are still relevant because most protein−carbohydrate interactions rely on multivalency and avidity effects to achieve sufficient binding

affinity. Both factors should play a role in DBPA-mediated interactions with GAGs.

Although the GAG-binding site composed of the linker residues and the C-terminus is the highest-affinity site on DBPA, titrations with conventional GAG ligands have also revealed that the N-terminus may be a weaker secondary binding site. These interactions are manifested in the significant chemical shift changes in atoms from N-terminal residues T28 and T101 during heparin dp6 titrations (Figure 3). However, K_D fitting showed that the dissociation constant of the binding is much weaker than that of residues located in the high-affinity site [3 mM vs 0.5 mM (Figure 9 of the Supporting Information)], and mutations at the main site left the K_D at the N-terminal site unchanged, indicating the N-terminal site is independent of the main GAG-binding site. The catalyst of these interactions is most likely a cluster of basic amino acids at the N-terminus, including R34, K102, and K104. The helical conformation of the segment allowed them to form a basic strip at the N-terminus that offers optimal geometry for interaction with GAGs. HSQCs of Arg side chain Hε−Nε showed the side chain of R34 experienced significant changes in chemical shift and signal intensity in the presence of heparin dp6 fragments (data not shown). This provides further proof that the N-terminus is involved in GAG binding. Although it has a weaker affinity than the main GAG-binding site, the secondary binding site may still offer significant contributions to DBPA's interactions with native GAG polymers *in vivo*.

■ ASSOCIATED CONTENT

Supporting Information

SDS−PAGE analysis of sample purity, GMSA analysis of DS d6−DBPA interaction, scheme for the reductive amination of heparin fragments, fittings of K_D values for heparin−DBPA interactions, ITC titrations of DBPAs with heparin dp6, and multisequence alignment of DBPAs from different strains of *B. burgdorferi*. This material is available free of charge via the Internet at http://pubs.acs.org.

■ AUTHOR INFORMATION

Corresponding Author

*Department of Chemistry & Biochemistry, Arizona State University, Tempe, AZ 85287. E-mail: xuwang@asu.edu. Phone: (480) 727-8256.

Funding

This research is supported by a grant from the National Institute of General Medical Sciences' K99/R00 program (5R00GM088483) and funds from Arizona State University.

Notes

The authors declare no competing financial interest.

■ ACKNOWLEDGMENTS

We thank Dr. Brian Cherry for the maintenance of spectrometers and Dr. Andrey Bobokov of Sanford-Burnham Medical Research Institute for performing the ITC titrations.

■ ABBREVIATIONS

DBP, decorin-binding protein; DBPA, decorin-binding protein A; DBPB, decorin-binding protein B; GAG, glycosaminoglycan; GMSA, gel mobility shift assay; ITC, isothermal titration calorimetry; HSQC, heteronuclear single-quantum coherence; PRE, paramagnetic relaxation enhancement; SAX, strong anion exchange; SDS−PAGE, sodium dodecyl sulfate−polyacrylamide gel electrophoresis.

■ REFERENCES

(1) Krupka, M., Zachova, K., Weigl, E., and Raska, M. (2011) Prevention of Lyme Disease: Promising Research or Sisyphean Task? *Arch. Immunol. Ther. Exp. 59*, 261−275.

(2) Fallon, B. A., Levin, E. S., Schweitzer, P. J., and Hardesty, D. (2010) Inflammation and central nervous system Lyme disease. *Neurobiol. Dis. 37*, 534−541.

(3) Halperin, J. J. (1998) Nervous system Lyme disease. *J. Neurol. Sci. 153*, 182−191.

(4) Schuijt, T. J., Hovius, J. W., van der Poll, T., van Dam, A. P., and Fikrig, E. (2011) Lyme borreliosis vaccination: The facts, the challenge, the future. *Trends Parasitol. 27*, 40−47.

(5) Guo, B. P., Brown, E. L., Dorward, D. W., Rosenberg, L. C., and Hook, M. (1998) Decorin-binding adhesins from *Borrelia burgdorferi*. *Mol. Microbiol. 30*, 711−723.

(6) Guo, B. P., Norris, S. J., Rosenberg, L. C., and Hook, M. (1995) Adherence of *Borrelia burgdorferi* to the proteoglycan decorin. *Infect. Immun. 63*, 3467−3472.

(7) Leong, J. M., Wang, H., Magoun, L., Field, J. A., Morrissey, P. E., Robbins, D., Tatro, J. B., Coburn, J., and Parveen, N. (1998) Different classes of proteoglycans contribute to the attachment of *Borrelia burgdorferi* to cultured endothelial and brain cells. *Infect. Immun. 66*, 994−999.

(8) Parveen, N., Robbins, D., and Leong, J. M. (1999) Strain variation in glycosaminoglycan recognition influences cell-type-specific binding by lyme disease spirochetes. *Infect. Immun. 67*, 1743−1749.

(9) Brown, E. L., Wooten, R. M., Johnson, B. J., Iozzo, R. V., Smith, A., Dolan, M. C., Guo, B. P., Weis, J. J., and Hook, M. (2001) Resistance to Lyme disease in decorin-deficient mice. *J. Clin. Invest. 107*, 845−852.

(10) Shi, Y., Xu, Q., McShan, K., and Liang, F. T. (2008) Both decorin-binding proteins A and B are critical for the overall virulence of *Borrelia burgdorferi*. *Infect. Immun. 76*, 1239−1246.

(11) Weening, E. H., Parveen, N., Trzeciakowski, J. P., Leong, J. M., Hoeoek, M., and Skare, J. T. (2008) *Borrelia burgdorferi* Lacking DbpBA Exhibits an Early Survival Defect during Experimental Infection. *Infect. Immun. 76*, 5694−5705.

(12) Blevins, J. S., Hagman, K. E., and Norgard, M. V. (2008) Assessment of decorin-binding protein A to the infectivity of *Borrelia burgdorferi* in the murine models of needle and tick infection. *BMC Microbiol. 8*, 82.

(13) Shi, Y., Xu, Q., Seemanaplli, S. V., McShan, K., and Liang, F. T. (2008) Common and unique contributions of decorin-binding proteins A and B to the overall virulence of *Borrelia burgdorferi*. *PLoS One 3*, e3340.

(14) Fischer, J. R., Parveen, N., Magoun, L., and Leong, J. M. (2003) Decorin-binding proteins A and B confer distinct mammalian cell type-specific attachment by *Borrelia burgdorferi*, the Lyme disease spirochete. *Proc. Natl. Acad. Sci. U.S.A. 100*, 7307−7312.

(15) Parveen, N., Caimano, M., Radolf, J. D., and Leong, J. M. (2003) Adaptation of the Lyme disease spirochaete to the mammalian host environment results in enhanced glycosaminoglycan and host cell binding. *Mol. Microbiol. 47*, 1433−1444.

(16) Benoit, V. M., Fischer, J. R., Lin, Y. P., Parveen, N., and Leong, J. M. (2011) Allelic variation of the Lyme disease spirochete adhesin DbpA influences spirochetal binding to decorin, dermatan sulfate, and mammalian cells. *Infect. Immun. 79*, 3501−3509.

(17) Wang, X. (2012) Solution structure of decorin-binding protein A from *Borrelia burgdorferi*. *Biochem. J. 51*, 8353−8362.

(18) Leong, J. M., Robbins, D., Rosenfeld, L., Lahiri, B., and Parveen, N. (1998) Structural requirements for glycosaminoglycan recognition by the Lyme disease spirochete, *Borrelia burgdorferi*. *Infect. Immun. 66*, 6045−6048.

(19) Brown, E. L., Guo, B. P., O'Neal, P., and Hook, M. (1999) Adherence of *Borrelia burgdorferi*. Identification of critical lysine

residues in DbpA required for decorin binding. *J. Biol. Chem. 274*, 26272−26278.
(20) Wang, X. (2012) Solution structure of decorin-binding protein A from *Borrelia burgdorferi*. *Biochemistry 51*, 8353−8362.
(21) Catanzariti, A. M., Soboleva, T. A., Jans, D. A., Board, P. G., and Baker, R. T. (2004) An efficient system for high-level expression and easy purification of authentic recombinant proteins. *Protein Sci. 13*, 1331−1339.
(22) Xiao, Z., Zhao, W., Yang, B., Zhang, Z., Guan, H., and Linhardt, R. J. (2011) Heparinase 1 selectivity for the 3,6-di-O-sulfo-2-deoxy-2-sulfamido-α-D-glucopyranose (1,4) 2-O-sulfo-α-L-idopyranosyluronic acid (GlcNS3S6S-IdoA2S) linkages. *Glycobiology 21*, 13−22.
(23) Lyon, M., Deakin, J. A., Lietha, D., Gherardi, E., and Gallagher, J. T. (2004) The Interactions of Hepatocyte Growth Factor/Scatter Factor and Its NK1 and NK2 Variants with Glycosaminoglycans Using a Modified Gel Mobility Shift Assay. *J. Biol. Chem. 279*, 43560−43567.
(24) Seo, E. S., Blaum, B. S., Vargues, T., De Cecco, M., Deakin, J. A., Lyon, M., Barran, P. E., Campopiano, D. J., and Uhrin, D. (2010) Interaction of human β-defensin 2 (HBD2) with glycosaminoglycans. *Biochemistry 49*, 10486−10495.
(25) Farmer, B. T., II, Constantine, K. L., Goldfarb, V., Friedrichs, M. S., Wittekind, M., Yanchunas, J., Jr., Robertson, J. G., and Mueller, L. (1996) Localizing the $NADP^+$ binding site on the MurB enzyme by NMR. *Nat. Struct. Biol. 3*, 995−997.
(26) Iwahara, J., Tang, C., and Marius Clore, G. (2007) Practical aspects of ^1H transverse paramagnetic relaxation enhancement measurements on macromolecules. *J. Magn. Reson. 184*, 185−195.
(27) Delaglio, F., Grzesiek, S., Vuister, G. W., Zhu, G., Pfeifer, J., and Bax, A. (1995) Nmrpipe: A Multidimensional Spectral Processing System Based on Unix Pipes. *J. Biomol. NMR 6*, 277−293.
(28) Johnson, B. A. (2004) Using NMRView to visualize and analyze the NMR spectra of macromolecules. *Methods Mol. Biol. 278*, 313−352.
(29) d'Auvergne, E. J., and Gooley, P. R. (2008) Optimisation of NMR dynamic models I. Minimisation algorithms and their performance within the model-free and Brownian rotational diffusion spaces. *J. Biomol. NMR 40*, 107−119.
(30) Kay, L. E., Torchia, D. A., and Bax, A. (1989) Backbone dynamics of proteins as studied by ^{15}N inverse detected heteronuclear NMR spectroscopy: Application to staphylococcal nuclease. *Biochemistry 28*, 8972−8979.
(31) Pikas, D. S., Brown, E. L., Gurusiddappa, S., Lee, L. Y., Xu, Y., and Hook, M. (2003) Decorin-binding sites in the adhesin DbpA from *Borrelia burgdorferi*: A synthetic peptide approach. *J. Biol. Chem. 278*, 30920−30926.
(32) Lis, H., and Sharon, N. (1998) Lectins: Carbohydrate-Specific Proteins That Mediate Cellular Recognition. *Chem. Rev. 98*, 637−674.
(33) Gemma, E., Hulme, A. N., Jahnke, A., Jin, L., Lyon, M., Muller, R. M., and Uhrin, D. (2007) DMT-MM mediated functionalisation of the non-reducing end of glycosaminoglycans. *Chem. Commun.*, 2686−2688.
(34) Jain, N. U., Venot, A., Umemoto, K., Leffler, H., and Prestegard, J. H. (2001) Distance mapping of protein-binding sites using spin-labeled oligosaccharide ligands. *Protein Sci. 10*, 2393−2400.
(35) Lipari, G., and Szabo, A. (1982) Model-Free Approach to the Interpretation of Nuclear Magnetic Resonance Relaxation in Macromolecules. 1. Theory and Range of Validity. *J. Am. Chem. Soc. 104*, 4546−4559.
(36) Lipari, G., and Szabo, A. (1982) Model-Free Approach to the Interpretation of Nuclear Magnetic Resonance Relaxation in Macromolecules. 2. Analysis of Experimental Results. *J. Am. Chem. Soc. 104*, 4559−4570.
(37) Imai, D. M., Samuels, D. S., Feng, S., Hodzic, E., Olsen, K., and Barthold, S. W. (2013) The early dissemination defect attributed to disruption of decorin-binding proteins is abolished in chronic murine lyme borreliosis. *Infect. Immun. 81*, 1663−1673.
(38) Chan, K., Awan, M., Barthold, S. W., and Parveen, N. (2012) Comparative molecular analyses of *Borrelia burgdorferi sensu stricto* strains B31 and N40D10/E9 and determination of their pathogenicity. *BMC Microbiol. 12*, 157.
(39) Varki, A. (2009) *Essentials of glycobiology*, 2nd ed., Cold Spring Harbor Laboratory Press, Plainview, NY.
(40) Takemoto, D. K., Skehel, J. J., and Wiley, D. C. (1996) A surface plasmon resonance assay for the binding of influenza virus hemagglutinin to its sialic acid receptor. *Virology 217*, 452−458.
(41) Probert, F., Whittaker, S. B., Crispin, M., Mitchell, D. A., and Dixon, A. M. (2013) Solution NMR Analyses of the C-type Carbohydrate Recognition Domain of DC-SIGNR Protein Reveal Different Binding Modes for HIV-derived Oligosaccharides and Smaller Glycan Fragments. *J. Biol. Chem. 288*, 22745−22757.